Phase-controlled robust quantum entanglement of remote mechanical oscillators

Jing-Xue Liu [1], Jian-Yong Yang,[1] Tian-Xiang Lu,[2] Ya-Feng Jiao,[3,4,*] and Hui Jing [1,4,†]

[1]*Key Laboratory of Low-Dimensional Quantum Structures and Quantum Control of Ministry of Education,*
Department of Physics and Synergetic Innovation Center for Quantum Effects and Applications,
Hunan Normal University, Changsha 410081, China
[2]*College of Physics and Electronic Information, Gannan Normal University, Ganzhou 341000, Jiangxi, China*
[3]*School of Electronics and Information, Zhengzhou University of Light Industry, Zhengzhou 450001, China*
[4]*Academy for Quantum Science and Technology, Zhengzhou University of Light Industry, Zhengzhou 450002, China*

Quantum entanglement between distant massive mechanical oscillators has played a central role in building and engineering quantum devices for application in long-distance quantum communications, distributed quantum sensing, and synchronized quantum processing. Here we propose to control quantum entanglement of two spatially separated mechanical oscillators in a cascaded quantum system by applying two counterpropagating pump fields. In particular, we find that by adjusting the phase difference of pump lasers, quantum entanglement between such two mechanical oscillators can be significantly enhanced, together with improved robustness against environmental thermal noise. Our work opens up a well-accessible way to manipulate and protect mechanical entanglement, shedding light on a wide range of practical applications requiring robust purely quantum resources.

I. INTRODUCTION

Cavity optomechanics (COM), utilizing radiation-pressure-mediated light-motion couplings [1–8], has experienced rapid advances in recent years due to its widespread applications in coherent microwave-to-light conversion [9–11], quantum COM sensing [12–18], and preparing purely quantum states of photons or phonons [19–21], to name only a few. In a recent experiment, macroscopic quantum correlations were even observed between laser and a 40 kg mirror at room temperature [22]. COM-based quantum entanglement [23–29], a unique resource in diverse quantum technologies, has also been demonstrated for optical fields [30,31] and various mechanical oscillators [32–40]. In particular, quantum entanglement between distant macroscopic mechanical objects was achieved [36–39], which is a crucial step towards important goals such as long-distance quantum communications [41–43], distributed quantum sensing [44–46], and synchronized quantum processing [47–49]. However, quantum entanglement is generally weak and easily destroyed by random noise and thus it is highly desirable to enhance and protect quantum-mechanical entanglement in practice.

In this paper, we propose to control and enhance quantum entanglement of two spatially separated mechanical oscillators in a cascaded quantum COM system by applying two counterpropagating pump lasers. We note that by tuning the phase difference of two pump lasers, one-way optical

transmission was demonstrated in recent experiments [50,51]. Such a strategy was also utilized to realize photon blockade [52,53], optical nonreciprocity [54,55], and particularly COM entanglement [56,57]. Inspired by these works, here we show that this strategy can also be applied to enhance and protect quantum entanglement between two spatially separated oscillators. We find that by adjusting the phase difference of pump lasers, quantum entanglement between two such mechanical oscillators can be significantly enhanced, together with improved robustness against environmental thermal noise. Our findings, well within the ability of current experiments and well compatible with other existing ways to protect quantum entanglement [58–68], shed light on making various phase-controlled quantum COM systems for applications in quantum information technologies.

This paper is organized as follows: In Sec. II, we introduce the model of our cascaded COM system and study its quantum dynamics in details. In Sec. III, we explore the phase-controlled entanglement between distant mechanical oscillators and examine its robustness against thermal noise. Finally a brief summary is given in Sec. IV.

II. PHASE-CONTROLLED CASCADED CAVITY OPTOMECHANICS SYSTEM: QUANTUM DYNAMICS

In this paper, we propose how to achieve coherent control and enhancement of the entanglement between two remote mechanical oscillators. Specifically, as shown in Fig. 1(a), we consider a bidirectional cascaded COM system consisting of two spatially separated Fabry-Pérot (FP) cavities and two telecommunication fibers. Each FP cavity has a fixed mirror and a movable mirror, thus supporting a pair of localized optical and mechanical modes with fundamental frequencies

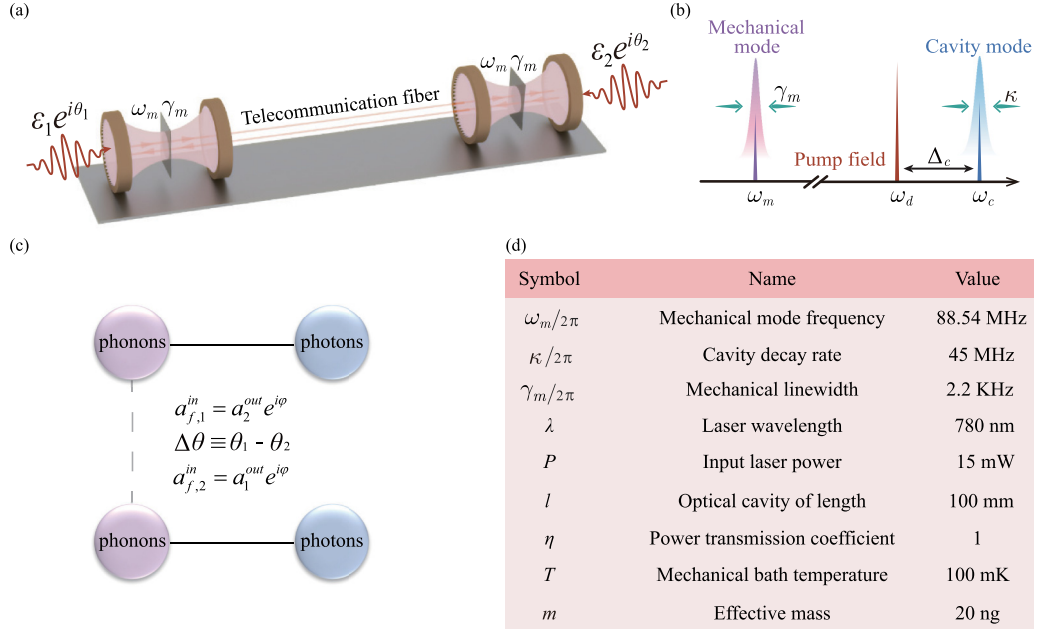*yfjiao91@foxmail.com
†jinghui73@gmail.com

FIG. 1. Robust entanglement between two long-distance mechanical oscillators. (a) Schematic diagram of a unidirectional cascaded COM system composed of two spatially distant FP cavities and two telecommunication fibers. Each FP cavity supports an optical mode and a mechanical mode, which are coupled through optical-radiation-pressure-mediated interactions. (b) Frequency spectrum of the cascaded COM system in panel (a). (c) Cartoon diagram of the interaction between photons and phonons. (d) The parameters chosen for our numerical calculations are experimentally feasible, which are partially selected from Refs. [69–73].

ω_c and ω_m, respectively. The two COM resonators are assumed to have neither direct acoustic interaction nor near-field optical couplings, and their cavity modes couple to each other indirectly by the light field propagating in the fiber. In a frame rotating at the driving frequency ω_d, the effective Hamiltonian of this cascaded COM system can be written as

$$\hat{H} = \hat{H}_0 + \hat{H}_{\text{int}} + \hat{H}_{\text{dr}},$$
$$\hat{H}_0 = \hbar\Delta_c\hat{a}_1^\dagger\hat{a}_1 + \hbar\Delta_c\hat{a}_2^\dagger\hat{a}_2 + \hbar\omega_m\hat{b}_1^\dagger\hat{b}_1 + \hbar\omega_m\hat{b}_2^\dagger\hat{b}_2,$$
$$\hat{H}_{\text{int}} = -\hbar g_0\hat{a}_1^\dagger\hat{a}_1(\hat{b}_1^\dagger + \hat{b}_1) - \hbar g_0\hat{a}_2^\dagger\hat{a}_2(\hat{b}_2^\dagger + \hat{b}_2),$$
$$\hat{H}_{\text{dr}} = i\hbar(\varepsilon_1\hat{a}_1^\dagger e^{-i\theta_1} + \varepsilon_2\hat{a}_2^\dagger e^{-i\theta_2} - \text{H.c.}), \quad (1)$$

where $\hat{a}_j$ $(\hat{a}_j^\dagger)$ and $\hat{b}_j$ $(\hat{b}_j^\dagger)$ $(j = 1, 2)$ are the annihilation (creation) operators of the optical and mechanical modes, respectively. $\Delta_c = \omega_c - \omega_d$ denotes the optical detuning between the cavity mode and the driving field. Also, $g_0 = (\omega_c/l)\sqrt{\hbar/m\omega_m}$ denotes the single-photon COM coupling strength, with an effective mass m and cavity length l. The phase and amplitude of the driving fields are given by θ_j and $|\varepsilon_j| = \sqrt{2\kappa P/\hbar\omega_d}$, where P is referred to as the input laser power of the driving fields, and κ denotes the optical decay rate. The vacuum input noise associated with the driven laser have been included in the κ (see such treatments also in Refs. [74–77]). The phase difference of the two pump lasers is defined by $\Delta\theta \equiv \theta_1 - \theta_2$. Robust entanglement between distant mechanical oscillators can be controlled by tuning this phase difference $\Delta\theta$.

Considering the influence of system dissipations and environmental input noise, the dynamic evolutions of the system can be completely described by the quantum Langevin

equations (QLEs) as

$$\dot{\hat{a}}_j = -(i\Delta_c + \kappa)\hat{a}_j + ig_0\hat{a}_j(\hat{b}_j^\dagger + \hat{b}_j) + \varepsilon_j e^{-i\theta_j}$$
$$+ \sqrt{2\eta\kappa}\hat{a}_{f,j}^{\text{in}} + \sqrt{2\kappa}\hat{a}_j^{\text{in}},$$
$$\dot{\hat{b}}_j = -(i\omega_m + \gamma_m)\hat{b}_j + ig_0\hat{a}_j^\dagger\hat{a}_j + \sqrt{2\gamma_m}\hat{b}_j^{\text{in}}, \quad (2)$$

where κ and γ_m are the optical decay rate and the mechanical damping rate, respectively. $\hat{a}_j^{\text{in}}$ and $\hat{b}_j^{\text{in}}$ denote the input vacuum noise operators for the optical and mechanical modes, which have zero-mean values and are characterized by the following correlation functions [78]:

$$\langle\hat{a}_j^{\text{in}}(t)\hat{a}_{j'}^{\text{in},\dagger}(t')\rangle = \delta_{jj'}\delta(t - t'),$$
$$\langle\hat{b}_j^{\text{in}}(t)\hat{b}_{j'}^{\text{in},\dagger}(t')\rangle = (n_{m,j} + 1)\delta_{jj'}\delta(t - t'),$$
$$\langle\hat{b}_j^{\text{in},\dagger}(t)\hat{b}_{j'}^{\text{in}}(t')\rangle = n_{m,j}\delta_{jj'}\delta(t - t'), \quad (3)$$

where $n_{m,j} = [\exp(\hbar\omega_m/k_BT) - 1]^{-1}$ is the mean thermal excitation number of the mechanical mode, k_B denotes the Boltzmann constant, and T is the bath temperature of the mechanical mode. For our bidirectional cascaded system, the operator $\hat{a}_{f,1}^{\text{in}}$ denotes the input field of the first cavity, and the operator $\hat{a}_{f,2}^{\text{in}}$ denotes that of the second cavity. As shown in Fig. 1(a), the laser driven from the 1st cavity excites the optical mode of the first cavity and then couples out of the cavity to the fiber, leading to the output field $\hat{a}^{\text{out}}$ which is in turn injected into the second cavity after propagating for a distance in the fiber. Consequently, this injected light (from the former cavity) can excite the optical mode of the second cavity. In contrast, this left-to-right order is reversed when driving the system from the opposite direction (i.e., the output

field $\hat{a}_2^{\text{out}}$ of the second cavity is injected into the first cavity), see also Ref. [40]. Based on this property of the bidirectional cascaded systems [79–84] and the input-output relations, we have

$$\hat{a}_{f,1}^{\text{in}} = \hat{a}_2^{\text{out}} e^{i\varphi}, \quad \hat{a}_{f,2}^{\text{in}} = \hat{a}_1^{\text{out}} e^{i\varphi},$$

$$\hat{a}_1^{\text{out}} = \varepsilon_1 e^{-i\theta_1} - \sqrt{2\kappa}\hat{a}_1,$$

$$\hat{a}_2^{\text{out}} = \varepsilon_2 e^{-i\theta_2} - \sqrt{2\kappa}\hat{a}_2, \tag{4}$$

where the phase φ is the cumulative phase delay caused by the propagation of light between the two FP cavities, which is given by

$$\varphi \equiv \omega_d t = 2\pi \frac{nL}{\lambda}, \tag{5}$$

where t is the propagating time, and L is the length of the fibers between the two FP cavities. Moreover, $\eta \in [0, 1]$ accounts for the imperfect couplings between the two FP cavities. The parameter $\eta = 1$ corresponds to a lossless unidirectional coupling between the two FP cavities, whereas $\eta = 0$ describes two independent FP cavities.

The dynamics of QLEs (2) involve the nonlinear COM interactions, and thus it is difficult to solve directly. Under the conditions of the strong driving fields, an arbitrary operator for this cascaded COM system can be expanded into the form of the sum of the steady-state mean and a small quantum fluctuation around it, i.e.,

$$\hat{a}_j = \alpha_j + \delta\hat{a}_j, \quad \hat{b}_j = \beta_j + \delta\hat{b}_j. \tag{6}$$

By substituting Eq. (6) into Eq. (2) based on the above assumptions, the first-order inhomogeneous differential equations can be obtained for steady-state mean values, i.e.,

$$\dot{\alpha}_1 = -(i\Delta + \kappa)\alpha_1 + \varepsilon_1 e^{-i\theta_1}$$
$$+ \sqrt{2\eta\kappa}\{\varepsilon_2 e^{-i\theta_2} - \sqrt{2\kappa}\alpha_2\}e^{i\varphi},$$

$$\dot{\alpha}_2 = -(i\Delta + \kappa)\alpha_2 + \varepsilon_2 e^{-i\theta_2}$$
$$+ \sqrt{2\eta\kappa}\{\varepsilon_1 e^{-i\theta_1} - \sqrt{2\kappa}\alpha_1\}e^{i\varphi},$$

$$\dot{\beta}_j = -(i\omega_m + \gamma_m)\beta_j + ig_0|\alpha_j|^2, \tag{7}$$

where $\Delta = \Delta_c - g_0(\beta_j^* + \beta_j)$ is the effective optical detuning. The corresponding linearized QLEs for quantum fluctuations are given by

$$\delta\dot{\hat{a}}_1 = -(i\Delta + \kappa)\delta\hat{a}_1 + ig_0\alpha_1(\delta\hat{b}_1^\dagger + \delta\hat{b}_1)$$
$$- 2\kappa\sqrt{\eta}e^{i\varphi}\delta\hat{a}_2 + \sqrt{2\kappa}\hat{a}_1^{in},$$

$$\delta\dot{\hat{a}}_2 = -(i\Delta + \kappa)\delta\hat{a}_2 + ig_0\alpha_2(\delta\hat{b}_2^\dagger + \delta\hat{b}_2)$$
$$- 2\kappa\sqrt{\eta}e^{i\varphi}\delta\hat{a}_1 + \sqrt{2\kappa}\hat{a}_2^{in},$$

$$\delta\dot{\hat{b}}_j = -(i\omega_m + \gamma_m)\delta\hat{b}_j + ig_0(\alpha_j^*\delta\hat{a}_j + \alpha_j\delta\hat{a}_j^\dagger) + \sqrt{2\gamma_m}\hat{b}_j^{\text{in}}. \tag{8}$$

From the linearized QLEs above, one can obtain the corresponding linearized system Hamiltonian:

$$\hat{H}^{lin} = \Delta(\delta\hat{a}_1^\dagger\delta\hat{a}_1 + \delta\hat{a}_2^\dagger\delta\hat{a}_2) + \omega_m(\delta\hat{b}_1^\dagger\delta\hat{b}_1 + \delta\hat{b}_2^\dagger\delta\hat{b}_2)$$
$$- g_0(\alpha_1\delta\hat{a}_1^\dagger + \alpha_1^*\delta\hat{a}_1)(\delta\hat{b}_1^\dagger + \delta\hat{b}_1)$$
$$- g_0(\alpha_2\delta\hat{a}_2^\dagger + \alpha_2^*\delta\hat{a}_2)(\delta\hat{b}_2^\dagger + \delta\hat{b}_2)$$
$$- 2i\kappa\sqrt{\eta}\delta\hat{a}_1^\dagger\delta\hat{a}_2 e^{i\varphi} - 2i\kappa\sqrt{\eta}\delta\hat{a}_1\delta\hat{a}_2^\dagger e^{i\varphi}. \tag{9}$$

The optical and mechanical modes are coupled via two kinds of interactions: (i) a parametric down-conversion-type process characterized by $\delta\hat{a}_j^\dagger\delta\hat{b}_j^\dagger + \delta\hat{a}_j\delta\hat{b}_j$ and (ii) a beam-splitter-type process characterized by $\delta\hat{a}_j^\dagger\delta\hat{b}_j + \delta\hat{a}_j\delta\hat{b}_j^\dagger$:

$$\hat{H}_0^{\text{lin}} = \Delta(\delta\hat{a}_1^\dagger\delta\hat{a}_1 + \delta\hat{a}_2^\dagger\delta\hat{a}_2) + \omega_m(\delta\hat{b}_1^\dagger\delta\hat{b}_1 + \delta\hat{b}_2^\dagger\delta\hat{b}_2),$$

$$\hat{H}_i^{\text{lin}} = -g_0(\alpha_1\delta\hat{a}_1^\dagger + \alpha_1^*\delta\hat{a}_1)(\delta\hat{b}_1^\dagger + \delta\hat{b}_1)$$
$$- g_0(\alpha_2\delta\hat{a}_2^\dagger + \alpha_2^*\delta\hat{a}_2)(\delta\hat{b}_2^\dagger + \delta\hat{b}_2)$$
$$- 2i\kappa\sqrt{\eta}\delta\hat{a}_1^\dagger\delta\hat{a}_2 e^{i\varphi} - 2i\kappa\sqrt{\eta}\delta\hat{a}_1\delta\hat{a}_2^\dagger e^{i\varphi}. \tag{10}$$

In a rotating frame defined by the transformation operator $\hat{U}(t) = \exp(-i\hat{H}_0^{lin}t)$, the transformed linearized system Hamiltonian becomes

$$\hat{H}_I^{lin} = \hat{U}^\dagger(t)\hat{H}_i^{lin}\hat{U}(t),$$

$$\hat{H}_I^{lin} = -g_0\{\alpha_1\delta\hat{a}_1^\dagger\delta\hat{b}_1^\dagger e^{i(\Delta+\omega_m)t} + \alpha_1\delta\hat{a}_1^\dagger\delta\hat{b}_1 e^{i(\Delta-\omega_m)t}\}$$
$$- g_0\{\alpha_1^*\delta\hat{a}_1\delta\hat{b}_1^\dagger e^{-i(\Delta-\omega_m)t} + \alpha_1^*\delta\hat{a}_1\delta\hat{b}_1 e^{-i(\Delta+\omega_m)t}\}$$
$$- g_0\{\alpha_2\delta\hat{a}_2^\dagger\delta\hat{b}_2^\dagger e^{i(\Delta+\omega_m)t} + \alpha_2\delta\hat{a}_2^\dagger\delta\hat{b}_2 e^{i(\Delta-\omega_m)t}\}$$
$$- g_0\{\alpha_2^*\delta\hat{a}_2\delta\hat{b}_2^\dagger e^{-i(\Delta-\omega_m)t} + \alpha_2^*\delta\hat{a}_2\delta\hat{b}_2 e^{-i(\Delta+\omega_m)t}\}$$
$$- 2i\kappa\sqrt{\eta}\delta\hat{a}_1^\dagger\delta\hat{a}_2 e^{i\varphi} - 2i\kappa\sqrt{\eta}\delta\hat{a}_1\delta\hat{a}_2^\dagger e^{i\varphi}. \tag{11}$$

If $\Delta = \omega_m$, we have

$$\hat{H}_I^{lin} = -g_0\{\alpha_1\delta\hat{a}_1^\dagger\delta\hat{b}_1^\dagger e^{2i\omega_m t} + \alpha_1\delta\hat{a}_1^\dagger\delta\hat{b}_1\}$$
$$- g_0\{\alpha_1^*\delta\hat{a}_1\delta\hat{b}_1^\dagger + \alpha_1^*\delta\hat{a}_1\delta\hat{b}_1 e^{-2i\omega_m t}\}$$
$$- g_0\{\alpha_2\delta\hat{a}_2^\dagger\delta\hat{b}_2^\dagger e^{2i\omega_m t} + \alpha_2\delta\hat{a}_2^\dagger\delta\hat{b}_2\}$$
$$- g_0\{\alpha_2^*\delta\hat{a}_2\delta\hat{b}_2^\dagger + \alpha_2^*\delta\hat{a}_2\delta\hat{b}_2 e^{-2i\omega_m t}\}$$
$$- 2i\kappa\sqrt{\eta}\delta\hat{a}_1^\dagger\delta\hat{a}_2 e^{i\varphi} - 2i\kappa\sqrt{\eta}\delta\hat{a}_1\delta\hat{a}_2^\dagger e^{i\varphi}. \tag{12}$$

Discarding the high-frequency terms, we obtain

$$\hat{H}_I^{lin} \approx -g_0(\alpha_1\delta\hat{a}_1^\dagger\delta\hat{b}_1 + \alpha_1^*\delta\hat{a}_1\delta\hat{b}_1^\dagger)$$
$$- g_0(\alpha_2\delta\hat{a}_2^\dagger\delta\hat{b}_2 + \alpha_2^*\delta\hat{a}_2\delta\hat{b}_2^\dagger)$$
$$- 2i\kappa\sqrt{\eta}\delta\hat{a}_1^\dagger\delta\hat{a}_2 e^{i\varphi} - 2i\kappa\sqrt{\eta}\delta\hat{a}_1\delta\hat{a}_2^\dagger e^{i\varphi}. \tag{13}$$

If $\Delta = -\omega_m$, we have

$$\hat{H}_I^{lin} = -g_0\{\alpha_1\delta\hat{a}_1^\dagger\delta\hat{b}_1^\dagger + \alpha_1\delta\hat{a}_1^\dagger\delta\hat{b}_1 e^{-2i\omega_m t}\}$$
$$- g_0\{\alpha_1^*\delta\hat{a}_1\delta\hat{b}_1^\dagger e^{2i\omega_m t} + \alpha_1^*\delta\hat{a}_1\delta\hat{b}_1\}$$
$$- g_0\{\alpha_2\delta\hat{a}_2^\dagger\delta\hat{b}_2^\dagger + \alpha_2\delta\hat{a}_2^\dagger\delta\hat{b}_2 e^{-2i\omega_m t}\}$$
$$- g_0\{\alpha_2^*\delta\hat{a}_2\delta\hat{b}_2^\dagger e^{2i\omega_m t} + \alpha_2^*\delta\hat{a}_2\delta\hat{b}_2\}$$
$$- 2i\kappa\sqrt{\eta}\delta\hat{a}_1^\dagger\delta\hat{a}_2 e^{i\varphi} - 2i\kappa\sqrt{\eta}\delta\hat{a}_1\delta\hat{a}_2^\dagger e^{i\varphi}. \tag{14}$$

Discarding the high-frequency terms, we obtain

$$
\begin{aligned}
\hat{H}_{\mathrm{I}}^{lin} \approx &-g_0(\alpha_1 \delta\hat{a}_1^\dagger \delta\hat{b}_1^\dagger + \alpha_1^* \delta\hat{a}_1 \delta\hat{b}_1) \\
&- g_0(\alpha_2 \delta\hat{a}_2^\dagger \delta\hat{b}_2^\dagger + \alpha_2^* \delta\hat{a}_2 \delta\hat{b}_2) \\
&- 2i\kappa\sqrt{\eta}\,\delta\hat{a}_1^\dagger \delta\hat{a}_2 e^{i\varphi} - 2i\kappa\sqrt{\eta}\,\delta\hat{a}_1 \delta\hat{a}_2^\dagger e^{i\varphi}.
\end{aligned}
\tag{15}
$$

Therefore, $\Delta = \omega_m$ corresponds to the red-detuned regime, and $\Delta = -\omega_m$ corresponds to the blue-detuned regime.

Then, we can obtain the steady-state mean values of the optical and mechanical modes by setting all the derivatives in Eq. (7) as zero, which are given by

$$
\begin{aligned}
\alpha_1 &= \frac{\varepsilon_1 e^{-i\theta_1} + \sqrt{2\eta\kappa}\{\varepsilon_2 e^{-i\theta_2} - \sqrt{2\kappa}\alpha_2\}e^{i\varphi}}{i\Delta + \kappa}, \\
\alpha_2 &= \frac{\varepsilon_2 e^{-i\theta_2} + \sqrt{2\eta\kappa}\{\varepsilon_1 e^{-i\theta_1} - \sqrt{2\kappa}\alpha_1\}e^{i\varphi}}{i\Delta + \kappa}, \\
\beta_j &= \frac{ig_0|\alpha_j|^2}{i\omega_m + \gamma_m}.
\end{aligned}
\tag{16}
$$

Explicitly, $N_j \equiv |\alpha_j|^2$ denotes the intracavity photon number. It is seen that the value of N_j is determined not only by the cumulative phase delay φ but also by the phase difference $\Delta\theta$, which provides an efficient way to regulate the field intensity and the COM interaction coherently.

By defining the optical and mechanical quadrature fluctuation operators as

$$
\delta\hat{X}_{a,j} = \frac{1}{\sqrt{2}}(\delta\hat{a}_{a,j} + \delta\hat{a}_{a,j}^\dagger), \quad \delta\hat{Y}_{a,j} = \frac{i}{\sqrt{2}}(\delta\hat{a}_{a,j}^\dagger - \delta\hat{a}_{a,j}),
$$

$$
\delta\hat{X}_{b,j} = \frac{1}{\sqrt{2}}(\delta\hat{b}_{b,j} + \delta\hat{b}_{b,j}^\dagger), \quad \delta\hat{Y}_{b,j} = \frac{i}{\sqrt{2}}(\delta\hat{b}_{b,j}^\dagger - \delta\hat{b}_{b,j}),
\tag{17}
$$

and the associated input noise operators as

$$
\hat{X}_{a,j}^{in} = \frac{1}{\sqrt{2}}\big(\hat{a}_{a,j}^{in} + \hat{a}_{a,j}^{in,\dagger}\big), \quad \hat{Y}_{a,j}^{in} = \frac{i}{\sqrt{2}}\big(\hat{a}_{a,j}^{in,\dagger} - \hat{a}_{a,j}^{in}\big),
$$

$$
\hat{X}_{b,j}^{in} = \frac{1}{\sqrt{2}}\big(\hat{b}_{b,j}^{in} + \hat{b}_{b,j}^{in,\dagger}\big), \quad \hat{Y}_{b,j}^{in} = \frac{i}{\sqrt{2}}\big(\hat{b}_{b,j}^{in,\dagger} - \hat{b}_{b,j}^{in}\big),
\tag{18}
$$

the corresponding linearized QLEs can be written clearly in a compact form as

$$
\dot{u}(t) = Au(t) + v(t),
\tag{19}
$$

where u and v are vectors of the quadrature fluctuation operators and the input noise operators, respectively, which are defined by

$$
u^T(t) = (\delta\hat{X}_{a,1}, \delta\hat{Y}_{a,1}, \delta\hat{X}_{a,2}, \delta\hat{Y}_{a,2}, \delta\hat{X}_{b,1}, \delta\hat{Y}_{b,1}, \delta\hat{X}_{b,2}, \delta\hat{Y}_{b,2}),
$$

$$
v^T(t) = \big(\hat{X}_{a,1}^{in}, \hat{Y}_{a,1}^{in}, \hat{X}_{a,2}^{in}, \hat{Y}_{a,2}^{in}, \hat{X}_{b,1}^{in}, \hat{Y}_{b,1}^{in}, \hat{X}_{b,2}^{in}, \hat{Y}_{b,2}^{in}\big).
\tag{20}
$$

The corresponding coefficient matrix A is given by

$$
A = \begin{pmatrix}
-\kappa & \Delta & -J_{c,1} & J_{s,1} & -\Lambda_1^{im} & 0 & 0 & 0 \\
-\Delta & -\kappa & -J_{s,1} & -J_{c,1} & \Lambda_1^{re} & 0 & 0 & 0 \\
-J_{c,2} & J_{s,2} & -\kappa & \Delta & 0 & 0 & -\Lambda_2^{im} & 0 \\
-J_{s,2} & -J_{c,2} & -\Delta & -\kappa & 0 & 0 & \Lambda_2^{re} & 0 \\
0 & 0 & 0 & 0 & -\gamma_m & \omega_m & 0 & 0 \\
\Lambda_1^{re} & \Lambda_1^{im} & 0 & 0 & -\omega_m & -\gamma_m & 0 & 0 \\
0 & 0 & 0 & 0 & 0 & 0 & -\gamma_m & \omega_m \\
0 & 0 & \Lambda_2^{re} & \Lambda_2^{im} & 0 & 0 & -\omega_m & -\gamma_m
\end{pmatrix},
\tag{21}
$$

with the components

$$
\begin{aligned}
\Lambda_1^{re} &= 2g_0\mathrm{Re}[\alpha_1], \quad \Lambda_1^{im} = 2g_0\mathrm{Im}[\alpha_1], \\
\Lambda_2^{re} &= 2g_0\mathrm{Re}[\alpha_2], \quad \Lambda_2^{im} = 2g_0\mathrm{Im}[\alpha_2], \\
J_{c,1} &= J_{c,2} = 2\kappa\sqrt{\eta}\cos(\varphi), \\
J_{s,1} &= J_{s,2} = 2\kappa\sqrt{\eta}\sin(\varphi).
\end{aligned}
$$

Also, the solution of the linearized QLEs (19) can be obtained as

$$
\hat{u}(t) = \mathcal{M}(t)\hat{u}(0) + \int_0^t d\tau \mathcal{M}(\tau)\hat{v}(t - \tau),
\tag{22}
$$

where

$$
\mathcal{M}(t) = \exp(At).
\tag{23}
$$

The system is stable only when all real part of the eigenvalues of A is negative, as characterized by the Routh-Hurwitz criterion [85]. When all the stability conditions are fulfilled, we can obtain $\mathcal{M}(\infty) = 0$ in the steady state, and

$$
\hat{u}_i(\infty) = \int_0^\infty d\tau \sum_k \mathcal{M}_{ik}(\tau)\hat{v}_k(t - \tau).
\tag{24}
$$

Due to the linearized dynamics and the Gaussian nature of the quantum noise, the steady state of the quantum fluctuations of this system can finally evolve into a quadripartite zero-mean Gaussian state, which is fully characterized by an 8×8 correlation matrix (CM) V with its components

$$
V_{kl} = \langle \hat{u}_k(\infty)\hat{u}_l(\infty) + \hat{u}_l(\infty)\hat{u}_k(\infty)\rangle/2.
\tag{25}
$$

By substituting Eq. (24) into Eq. (25) and using the fact that the eight components of $\hat{v}(t)$ are not correlated with each

other, the steady-state CM V is obtained by

$$V = \int_0^\infty d\tau \, \mathcal{M}(\tau) D \mathcal{M}^{\mathrm{T}}(\tau), \tag{26}$$

where

$$D = \mathrm{Diag}[\kappa, \kappa, \kappa, \kappa, \gamma_m(2n_m + 1), \gamma_m(2n_m + 1),$$
$$\gamma_m(2n_m + 1), \gamma_m(2n_m + 1)] \tag{27}$$

is a diffusion matrix, which is obtained by using

$$\langle \hat{v}_k(\tau) \hat{v}_l(\tau') + \hat{v}_l(\tau') \hat{v}_k(\tau) \rangle / 2 = D_{kl} \delta(\tau - \tau'). \tag{28}$$

When the stability condition is satisfied, the dynamics of the steady-state CM V fulfills the Lyapunov equation [23]:

$$AV + VA^{\mathrm{T}} = -D. \tag{29}$$

Equation (29) is a linear equation and allows us to derive CM V for any values of the relevant parameters. However, the analytical expression of V is too complicated and thus is not reported here.

III. RESULTS AND DISCUSSIONS

For quantifying bipartite entanglement between the two mechanical modes in a multimode continuous variable system, we can adopt the logarithmic negativity E_N as an effective measure, which can be defined as [86]

$$E_{\mathrm{N}} = \max[0, -\ln(2\nu^-)], \tag{30}$$

where

$$\nu^- = 2^{-1/2}\{\Sigma(V') - [\Sigma(V')^2 - 4\det V']^{1/2}\}^{1/2}, \tag{31}$$

with

$$\Sigma(V') = \det\mathcal{A} + \det\mathcal{B} - 2\det\mathcal{C}. \tag{32}$$

Here, ν^- is the smallest symplectic eigenvalue of the partial transpose of a reduced 4×4 CM V'. The reduced CM V' contains the entries of V, and it can be directly derived by choosing the rows and columns of the interesting mode. The reduced CM V' can be obtained in a 2×2 block form,

$$V' = \begin{pmatrix} \mathcal{A} & \mathcal{C} \\ \mathcal{C}^{\mathrm{T}} & \mathcal{B} \end{pmatrix}. \tag{33}$$

Equation (30) indicates that the entanglement between the two mechanical modes can emerge only when $\nu^- < 1/2$, which is equivalent to Simon's necessary and sufficient entanglement nonpositive partial transpose criterion (or the related Peres-Horodecki criterion) for certifying entanglement of two-mode system in Gaussian states [87].

In this cascaded COM system, the optical and mechanical modes are coupled together through the optomechanical interaction. As shown in Fig. 1(a), two FP cavities are connected by the input-output relationships of driving fields in the telecommunication fibers [i.e., see Eq. (4)], forming an indirect coupling and interaction. This indirect interaction is well represented by the dotted line in Fig. 1(c). Therefore, the two mechanical modes are indirectly coupled together through the input-output relationships of driving fields in the telecommunication fibers, and there is an indirect interaction, which can induce entanglement between the two mechanical modes
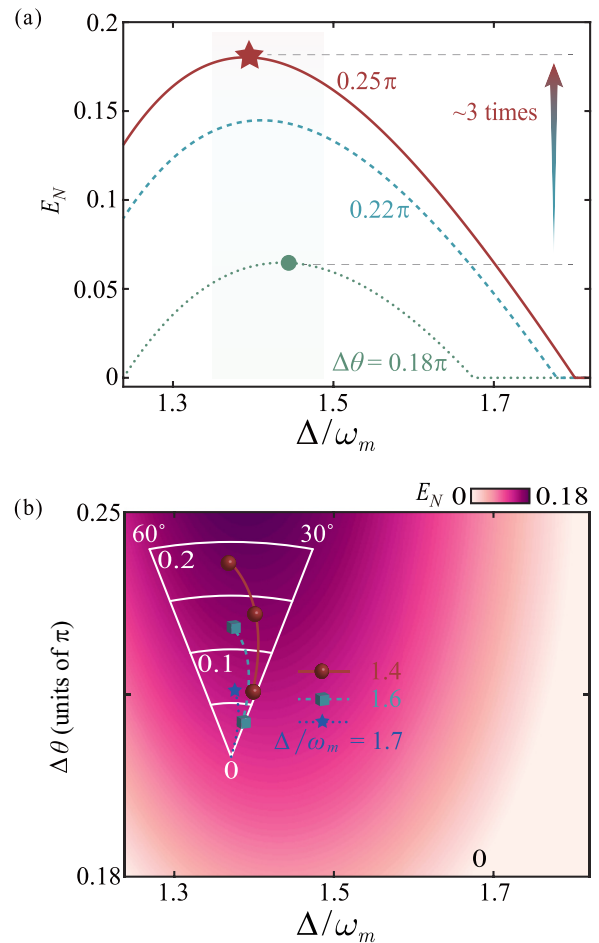

FIG. 2. Phase-controlled robust entanglement between two long-distance mechanical oscillators by tuning phase difference $\Delta\theta$ of driving fields. (a) The logarithmic negativity E_N versus the scaled optical detuning Δ/ω_m, with $\varphi = 0.8\pi$, and $\Delta\theta = 0.18\pi$, 0.22π, or 0.25π. Compared with the phase difference $\Delta\theta = 0.18\pi$, the maximum value of E_N can be enhanced for approximately three times through tuning phase difference $\Delta\theta = 0.25\pi$. (b) Density plot of the logarithmic negativity E_N as a function of the scaled optical detuning Δ/ω_m and the phase difference $\Delta\theta$. In the inset, E_N is plotted as a function of $\Delta\theta$ in polar coordinates with different values of Δ/ω_m.

(see also Ref. [40]). This is the source of entanglement in the cascaded COM system. As already confirmed in previous works, quantum entanglement created under the red-detuned condition is more stable than that in the blue-detuning regime (see, e.g., Ref. [24]).

In Fig. 2, we first explore how to regulate the behavior of the entanglement between the two mechanical oscillators by tuning the phase difference $\Delta\theta$ of the two driving lasers. In our numerical calculation, for ensuring the stability and experimental feasibility of this compound system, the parameters are moderately chosen for two identical FP cavities [69–73]: $\omega_m/2\pi = 88.54$ MHz, $\kappa/2\pi = 45$ MHz, $\gamma_m/2\pi = 2.2$ kHz, $\lambda = 780$ nm, $P = 15$ mW, $l = 100$ mm, $\eta = 1$, $\varphi = 0.8\pi$, $T = 100$ mK, and $m = 20$ ng. Specifically, as shown in Fig. 2(a), the logarithmic negativity E_N is plotted as a function of the scaled optical detuning Δ/ω_m for different values of the phase difference $\Delta\theta$. It is seen that the
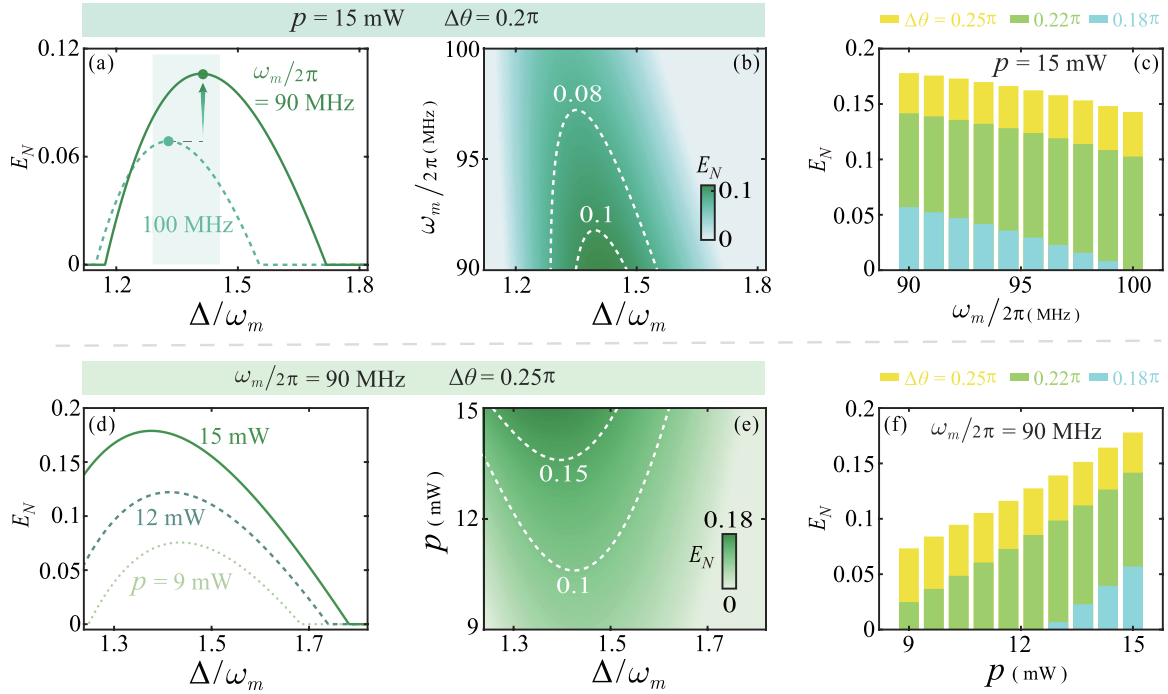
FIG. 3. The influence of the mechanical oscillator frequency and the input laser power on entanglement. (a) The logarithmic negativity E_N as a function of the scaled optical detuning Δ/ω_m for different mechanical oscillator frequencies ω_m. (b) Density plot of the logarithmic negativity E_N as a function of the mechanical oscillator frequency ω_m and the scaled optical detuning Δ/ω_m. Here we have chosen the phase difference $\Delta\theta = 0.2\pi$ and the input laser power $P = 15$ mW. Compared with the mechanical oscillator frequency $\omega_m/2\pi = 100$ MHz, the maximum value of E_N can be enhanced effectively by selecting the mechanical oscillator frequency $\omega_m/2\pi = 90$ MHz. (c) The logarithmic negativity E_N as a function of the mechanical oscillators frequency ω_m for different phase difference $\Delta\theta$ of driving fields. (d) The logarithmic negativity E_N as a function of the scaled optical detuning Δ/ω_m for different input laser power P. (e) Density plot of the logarithmic negativity E_N as a function of the input laser power P and the scaled optical detuning Δ/ω_m. Here we have chosen the phase difference $\Delta\theta = 0.25\pi$ and the mechanical oscillator frequency $\omega_m/2\pi = 90$ MHz. (f) The logarithmic negativity E_N as a function of the input laser power P for different phase difference $\Delta\theta$ of driving fields. The other parameters are selected as listed in the table of Fig. 1(d).

COM entanglement is present within a finite interval of Δ around $\Delta/\omega_m \simeq 1.4$. When tuning the phase difference $\Delta\theta$ of the driving fields, the logarithmic negativity E_N can be well modulated or even enhanced with respect to some specific values of phase difference $\Delta\theta$. For example, it is found that such mechanical entanglement can reach the maximum value for an optimal phase difference $\Delta\theta = 0.25\pi$, which is enhanced by about three times in comparison with that of the case $\Delta\theta = 0.18\pi$. To more clearly see this effect, we also show the dependence of the logarithmic negativity E_N on the scaled optical detuning Δ/ω_m and the phase difference $\Delta\theta$ in Fig. 2(b). It is seen that E_N is monotonically increasing with the increase of $\Delta\theta$ ranging from 0.18π to 0.25π. Besides, it should be stressed that, for other values of $\Delta\theta$, the system is unstable and thus entanglement cannot emerge in this case.

In Fig. 3, we further investigate the influence of the phase difference $\Delta\theta$ on mechanical entanglement generation for different values of mechanical frequencies ω_m and pump powers P. As shown in Figs. 3(a)–3(c), we first present the dependence of the logarithmic negativity E_N on phase difference $\Delta\theta$ and mechanical frequency ω_m, with $P = 15$ mW. It is seen that the profiles of E_N are characterized by sharp peaks with maximum values $E_N \simeq 0.11$ for $\omega_m/2\pi = 90$ MHz and $E_N \simeq 0.07$ for $\omega_m/2\pi = 100$ MHz [see Fig. 3(a)]. Also, for the same value of $\Delta\theta$ (e.g., $\Delta\theta = 0.2\pi$), the maximum value

of E_N tends to be suppressed when increasing the frequency of the mechanical oscillators [see Fig. 3(b)]. Figure 3(c) shows that, for the same value of mechanical frequency, E_N can be considerably enhanced by tuning phase difference $\Delta\theta$. These results indicate that when using mechanical oscillators with high frequencies, the mechanical entanglement is more difficult to be generated. However, by choosing a proper phase difference of the driving fields, the degree of mechanical entanglement can be improved, which is beneficial for the entanglement generation with high-frequency mechanical oscillators. In Figs. 3(d)–3(f), we show the dependence of the logarithmic negativity E_N on phase difference $\Delta\theta$ and the pump power P, with $\omega_m/2\pi = 90$ MHz. It is seen that by increasing the pump power P, the mechanical entanglement can be enhanced directly [see Figs. 3(d) and 3(e)]. Moreover, similar to the case we discussed above, when tuning the phase difference of the driving fields, one can further improve the mechanical entanglement [see Fig. 3(f)].

Finally, we show the influence of the phase difference $\Delta\theta$ on mechanical entanglement generation for different values of bath temperature T. For this purpose, we plot the logarithmic negativity E_N as a function of the bath temperature T in Fig. 4, with $\Delta\theta = \pi/5$ or $\pi/4$. The inserted figure shows the dependence of the logarithmic negativity E_N on bath temperature T and scaled optical detuning Δ/ω_m. It is seen that the mechanical entanglement is fragile to thermal noise, and it tends to be
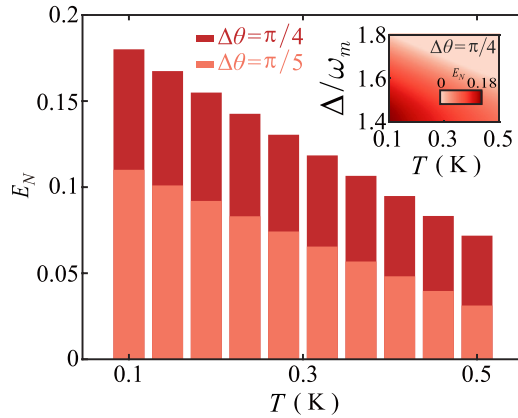
FIG. 4. The influence of thermal effects on entanglement. The logarithmic negativity E_N as a function of the environment temperature T for different phase difference $\Delta\theta$ of driving fields, with the scaled optical detuning $\Delta/\omega_m = 1.4$, in the panel. Density plot of the logarithmic negativity E_N as a function of the environment temperature T and the scaled optical detuning Δ/ω_m, with the phase difference $\Delta\theta = \pi/4$, in the inset.

destroyed when the bath temperature increases. However, it is also seen that, under the same condition of bath temperature T, the mechanical entanglement could become more robust to thermal noise with respect to some specific values of phase difference. Thus, our proposed scheme holds the promise to be useful for protecting the fragile entanglement from thermal noise.

IV. CONCLUSION

In summary, we have investigated how to generate and manipulate the entanglement between two distant mechanical oscillators through adjusting the phase difference of the driving lasers in a cascaded COM system. We find that, by tuning the phase difference of the driving lasers, one can significantly enhance the degree of the mechanical entanglement, as well as improve the robustness of such entanglement against thermal noise. Our work, shedding a light on protecting and improving the performance of various quantum devices in practical noisy environment, provides an opportunity to realize a number of entanglement-enabled quantum technology, such as quantum computing [88–90], quantum sensing [91–94], and quantum networking [95–98]. In a broader view, we envision that our work can be extended to study various other quantum effects based on cascaded systems, such as synchronization [80–82], squeezing [76,99], and photon blockade [77,100,101].

[1] T. J. Kippenberg and K. J. Vahala, Cavity opto-mechanics, Opt. Express **15**, 17172 (2007).

[2] E. Verhagen, S. Deléglise, S. Weis, A. Schliesser, and T. J. Kippenberg, Quantum-coherent coupling of a mechanical oscillator to an optical cavity mode, Nature (London) **482**, 63 (2012).

[3] M. Aspelmeyer, T. J. Kippenberg, and F. Marquardt, Cavity optomechanics, Rev. Mod. Phys. **86**, 1391 (2014).

[4] H. Xiong, L.-G. Si, X.-Y. Lü, X.-X. Yang, and Y. Wu, Review of cavity optomechanics in the weak-coupling regime: From linearization to intrinsic nonlinear interactions, Sci. China: Phys., Mech. Astron. **58**, 1 (2015).

[5] S. Barzanjeh, A. Xuereb, S. Gröblacher, M. Paternostro, C. A. Regal, and E. M. Weig, Optomechanics for quantum technologies, Nat. Phys. **18**, 15 (2022).

[6] B. Chen, Y. Guo, and H. Shen, Spontaneous phase locking of mechanical multimodes in anti-parity-time optomechanics, Opt. Express **28**, 28762 (2020).

[7] X.-W. Xu, J.-Q. Liao, H. Jing, and L.-M. Kuang, Anti-parity-time symmetry hidden in a damping linear resonator, Sci. China: Phys., Mech. Astron. **66**, 100312 (2023).

[8] J.-S. Tang, W. Nie, L. Tang, M. Chen, X. Su, Y. Lu, F. Nori, and K. Xia, Nonreciprocal single-photon band structure, Phys. Rev. Lett. **128**, 203602 (2022).

[9] R. Sahu, W. Hease, A. Rueda, G. Arnold, L. Qiu, and J. M. Fink, Quantum-enabled operation of a microwave-optical interface, Nat. Commun. **13**, 1276 (2022).

[10] M. Forsch, R. Stockill, A. Wallucks, I. Marinković, C. Gärtner, R. A. Norte, F. van Otten, A. Fiore, K. Srinivasan, and S. Gröblacher, Microwave-to-optics conversion using a mechanical oscillator in its quantum ground state, Nat. Phys. **16**, 69 (2020).

[11] S. Hönl, Y. Popoff, D. Caimi, A. Beccari, T. J. Kippenberg, and P. Seidler, Microwave-to-optical conversion with a gallium phosphide photonic crystal cavity, Nat. Commun. **13**, 2065 (2022).

[12] F. Massel, S. U. Cho, J.-M. Pirkkalainen, P. J. Hakonen, T. T. Heikkilä, and M. A. Sillanpää, Multimode circuit optomechanics near the quantum limit, Nat. Commun. **3**, 987 (2012).

[13] D. E. McClelland, N. Mavalvala, Y. Chen, and R. Schnabel, Advanced interferometry, quantum optics and optomechanics in gravitational wave detectors, Laser Photonics Rev. **5**, 677 (2011).

[14] S. Qvarfort, A. Serafini, P. F. Barker, and S. Bose, Gravimetry through non-linear optomechanics, Nat. Commun. **9**, 3690 (2018).

[15] W. Zhao, S.-D. Zhang, A. Miranowicz, and H. Jing, Weak-force sensing with squeezed optomechanics, Sci. China: Phys., Mech. Astron. **63**, 224211 (2020).

[16] C.-H. Dong, L. He, Y.-F. Xiao, V. R. Gaddam, Ş. K. Özdemir, Z.-F. Han, G.-C. Guo, and L. Yang, Fabrication of high-Q

polydimethylsiloxane optical microspheres for thermal sensing, Appl. Phys. Lett. **94**, 231119 (2009).

[17] H. Jing, H. Lü, Ş. K. Özdemir, T. Carmon, and F. Nori, Nanoparticle sensing with a spinning resonator, Optica **5**, 1424 (2018).

[18] Q. Zhong, J. Ren, M. Khajavikhan, D. N. Christodoulides, Ş. K. Özdemir, and R. El-Ganainy, Sensing with exceptional surfaces in order to combine sensitivity with robustness, Phys. Rev. Lett. **122**, 153902 (2019).

[19] B. Vermersch, P.-O. Guimond, H. Pichler, and P. Zoller, Quantum state transfer via noisy photonic and phononic waveguides, Phys. Rev. Lett. **118**, 133601 (2017).

[20] C.-W. Chou, C. Kurz, D. B. Hume, P. N. Plessow, D. R. Leibrandt, and D. Leibfried, Preparation and coherent manipulation of pure quantum states of a single molecular ion, Nature (London) **545**, 203 (2017).

[21] A. M. Barth, S. Lüker, A. Vagov, D. E. Reiter, T. Kuhn, and V. M. Axt, Fast and selective phonon-assisted state preparation of a quantum dot by adiabatic undressing, Phys. Rev. B **94**, 045306 (2016).

[22] H. Yu, L. McCuller, M. Tse, N. Kijbunchoo, L. Barsotti, N. Mavalvala, and L. S. Collaboration, Quantum correlations between light and the kilogram-mass mirrors of LIGO, Nature (London) **583**, 43 (2020).

[23] D. Vitali, S. Gigan, A. Ferreira, H. R. Böhm, P. Tombesi, A. Guerreiro, V. Vedral, A. Zeilinger, and M. Aspelmeyer, Optomechanical entanglement between a movable mirror and a cavity field, Phys. Rev. Lett. **98**, 030405 (2007).

[24] C. Genes, A. Mari, P. Tombesi, and D. Vitali, Robust entanglement of a micromechanical resonator with output optical fields, Phys. Rev. A **78**, 032316 (2008).

[25] R. Ghobadi, S. Kumar, B. Pepper, D. Bouwmeester, A. I. Lvovsky, and C. Simon, Optomechanical Micro-Macro entanglement Phys. Rev. Lett. **112**, 080503 (2014).

[26] Z.-Q. Liu, C.-S. Hu, Y.-K. Jiang, W.-J. Su, H. Wu, Y. Li, and S.-B. Zheng, Engineering optomechanical entanglement via dual-mode cooling with a single reservoir, Phys. Rev. A **103**, 023525 (2021).

[27] J. Li, S.-Y. Zhu, and G. S. Agarwal, Magnon-photon-phonon entanglement in cavity magnomechanics, Phys. Rev. Lett. **121**, 203601 (2018).

[28] T. M. Karg, B. Gouraud, C. T. Ngai, G.-L. Schmid, K. Hammerer, and P. Treutlein, Light-mediated strong coupling between a mechanical oscillator and atomic spins 1 meter apart, Science **369**, 174 (2020).

[29] Y. Li, Y.-F. Jiao, J.-X. Liu, A. Miranowicz, Y.-L. Zuo, L.-M. Kuang, and H. Jing, Vector optomechanical entanglement, Nanophotonics **11**, 67 (2021).

[30] S. Barzanjeh, E. S. Redchenko, M. Peruzzo, M. Wulf, D. P. Lewis, G. Arnold, and J. M. Fink, Stationary entangled radiation from micromechanical motion, Nature (London) **570**, 480 (2019).

[31] J. Chen, M. Rossi, D. Mason, and A. Schliesser, Entanglement of propagating optical modes via a mechanical interface, Nat. Commun. **11**, 943 (2020).

[32] S. Mancini, V. Giovannetti, D. Vitali, and P. Tombesi, Entangling macroscopic oscillators exploiting radiation pressure, Phys. Rev. Lett. **88**, 120401 (2002).

[33] S. Huang and G. S. Agarwal, Entangling nanomechanical oscillators in a ring cavity by feeding squeezed light, New J. Phys. **11**, 103044 (2009).

[34] H. Tan, L. F. Buchmann, H. Seok, and G. Li, Achieving steady-state entanglement of remote micromechanical oscillators by cascaded cavity coupling, Phys. Rev. A **87**, 022318 (2013).

[35] J. Li, I. M. Haghighi, N. Malossi, S. Zippilli, and D. Vitali, Generation and detection of large and robust entanglement between two different mechanical resonators in cavity optomechanics, New J. Phys. **17**, 103037 (2015).

[36] C. F. Ockeloen-Korppi, E. Damskägg, J.-M. Pirkkalainen, M. Asjad, A. A. Clerk, F. Massel, M. J. Woolley, and M. A. Sillanpää, Stabilized entanglement of massive mechanical oscillators, Nature (London) **556**, 478 (2018).

[37] R. Riedinger, A. Wallucks, I. Marinković, C. Löschnauer, M. Aspelmeyer, S. Hong, and S. Gröblacher, Remote quantum entanglement between two micromechanical oscillators, Nature (London) **556**, 473 (2018).

[38] L. Mercier de Lépinay, C. F. Ockeloen-Korppi, M. J. Woolley, and M. A. Sillanpää, Quantum mechanics-free subsystem with mechanical oscillators, Science **372**, 625 (2021).

[39] S. Kotler, G. A. Peterson, E. Shojaee, F. Lecocq, K. Cicak, A. Kwiatkowski, S. Geller, S. Glancy, E. Knill, R. W. Simmonds, J. Aumentado, and J. D. Teufel, Direct observation of deterministic macroscopic entanglement, Science **372**, 622 (2021).

[40] Y.-F. Jiao, J.-X. Liu, Y. Li, R. Yang, L.-M. Kuang, and H. Jing, Nonreciprocal enhancement of remote entanglement between nonidentical mechanical oscillators, Phys. Rev. Appl. **18**, 064008 (2022).

[41] A. Khalique and B. C. Sanders, Long-distance quantum communication through any number of entanglement-swapping operations, Phys. Rev. A **90**, 032304 (2014).

[42] X.-M. Hu, C.-X. Huang, Y.-B. Sheng, L. Zhou, B.-H. Liu, Y. Guo, C. Zhang, W.-B. Xing, Y.-F. Huang, C.-F. Li, and G.-C. Guo, Long-distance entanglement purification for quantum communication, Phys. Rev. Lett. **126**, 010503 (2021).

[43] A. Khalique, W. Tittel, and B. C. Sanders, Practical long-distance quantum communication using concatenated entanglement swapping, Phys. Rev. A **88**, 022336 (2013).

[44] B. K. Malia, Y. Wu, J. MartÍnez-Rincón, and M. A. Kasevich, Distributed quantum sensing with mode-entangled spin-squeezed atomic states, Nature (London) **612**, 661 (2022).

[45] X. Guo, C. R. Breum, J. Borregaard, S. Izumi, M. V. Larsen, T. Gehring, M. Christandl, J. S. Neergaard-Nielsen, and U. L. Andersen, Distributed quantum sensing in a continuous-variable entangled network, Nat. Phys. **16**, 281 (2020).

[46] Q. Zhuang, Z. Zhang, and J. H. Shapiro, Distributed quantum sensing using continuous-variable multipartite entanglement, Phys. Rev. A **97**, 032329 (2018).

[47] Q.-C. Sun, Y.-L. Mao, S.-J. Chen, W. Zhang, Y.-F. Jiang, Y.-B. Zhang, W.-J. Zhang, S. Miki, T. Yamashita, H. Terai, X. Jiang, T.-Y. Chen, L.-X. You, X.-F. Chen, Z. Wang, J.-Y. Fan, Q. Zhang, and J.-W. Pan, Quantum teleportation with independent sources and prior entanglement distribution over a network, Nat. Photon. **10**, 671 (2016).

[48] K. Makino, Y. Hashimoto, J. Yoshikawa, H. Ohdan, T. Toyama, P. van Loock, and A. Furusawa, Synchronization of optical photons for quantum information processing, Sci. Adv. **2**, e1501772 (2016).

[49] U. Yurtsever and J. P. Dowling, Lorentz-invariant look at quantum clock-synchronization protocols based on distributed entanglement, Phys. Rev. A **65**, 052317 (2002).

[50] Y. Chen, Y.-L. Zhang, Z. Shen, C.-L. Zou, G.-C. Guo, and C.-H. Dong, Synthetic gauge fields in a single optomechanical resonator, Phys. Rev. Lett. **126**, 123603 (2021).

[51] L. Ren, S. Yuan, S. Zhu, L. Shi, and X. Zhang, Backscattering-induced chiral absorption in optical microresonators, ACS Photon. **10**, 3797 (2023).

[52] X.-W. Xu, Y. Li, B. Li, H. Jing, and A.-X. Chen, Nonreciprocity via nonlinearity and synthetic magnetism, Phys. Rev. Appl. **13**, 044070 (2020).

[53] M. Li, Y.-L. Zhang, S.-H. Wu, C.-H. Dong, X.-B. Zou, G.-C. Guo, and C.-L. Zou, Single-mode photon blockade enhanced by Bi-tone drive, Phys. Rev. Lett. **129**, 043601 (2022).

[54] X.-B. Yan, H.-L. Lu, F. Gao, and L. Yang, Perfect optical non-reciprocity in a double-cavity optomechanical system, Front. Phys. **14**, 52601 (2019).

[55] X.-W. Xu and Y. Li, Optical nonreciprocity and optomechanical circulator in three-mode optomechanical systems, Phys. Rev. A **91**, 053854 (2015).

[56] J.-X. Liu, Y.-F. Jiao, Y. Li, X.-W. Xu, Q.-Y. He, and H. Jing, Phase-controlled asymmetric optomechanical entanglement against optical backscattering, Sci. China: Phys., Mech. Astron. **66**, 230312 (2023).

[57] F. X. Sun, D. Mao, Y. T. Dai, Z. Ficek, Q. Y. He, and Q. H. Gong, Phase control of entanglement and quantum steering in a three-mode optomechanical system, New J. Phys. **19**, 123039 (2017).

[58] M. C. Rechtsman, Y. Lumer, Y. Plotnik, A. Perez-Leija, A. Szameit, and M. Segev, Topological protection of photonic path entanglement, Optica **3**, 925 (2016).

[59] H. Zhou, T. Li, and K. Xia, Parallel and heralded multiqubit entanglement generation for quantum networks, Phys. Rev. A **107**, 022428 (2023).

[60] Y.-F. Jiao, S.-D. Zhang, Y.-L. Zhang, A. Miranowicz, L.-M. Kuang, and H. Jing, Nonreciprocal optomechanical entanglement against backscattering losses, Phys. Rev. Lett. **125**, 143605 (2020).

[61] C. Gneiting, D. Leykam, and F. Nori, Phys. Rev. Lett. **122**, 066601 (2019).

[62] D.-G. Lai, J.-Q. Liao, A. Miranowicz, and F. Nori, Noise-tolerant optomechanical entanglement via synthetic magnetism, Phys. Rev. Lett. **129**, 063602 (2022).

[63] M. Yu, H. Shen, and J. Li, Magnetostrictively induced stationary entanglement between two microwave fields, Phys. Rev. Lett. **124**, 213604 (2020).

[64] X.-Y. Lü, G.-L. Zhu, L.-L. Zheng, and Y. Wu, Entanglement and quantum superposition induced by a single photon, Phys. Rev. A **97**, 033807 (2018).

[65] D.-G. Lai, W. Qin, B.-P. Hou, A. Miranowicz, and F. Nori, Significant enhancement in refrigeration and entanglement in auxiliary-cavity-assisted optomechanical systems, Phys. Rev. A **104**, 043521 (2021).

[66] W. Qin, A. Miranowicz, P.-B. Li, X.-Y. Lü, J. Q. You, and F. Nori, Exponentially enhanced light-matter interaction, cooperativities, and steady-state entanglement using parametric amplification, Phys. Rev. Lett. **120**, 093601 (2018).

[67] M. Wang, X.-Y. Lü, Y.-D. Wang, J. Q. You, and Y. Wu, Macroscopic quantum entanglement in modulated optomechanics, Phys. Rev. A **94**, 053807 (2016).

[68] T. Li, Z. Wang, and K. Xia, Multipartite quantum entanglement creation for distant stationary systems, Opt. Express **28**, 1316 (2020).

[69] J. D. Thompson, B. M. Zwickl, A. M. Jayich, F. Marquardt, S. M. Girvin, and J. G. E. Harris, Strong dispersive coupling of a high finesse cavity to a micromechanical membrane, Nature (London) **452**, 72 (2008).

[70] S. Gröblacher, J. B. Hertzberg, M. R. Vanner, G. D. Cole, S. Gigan, K. C. Schwab, and M. Aspelmeyer, Demonstration of an ultracold micro-optomechanical oscillator in a cryogenic cavity, Nat. Phys. **5**, 485 (2009).

[71] I. Galinskiy, Y. Tsaturyan, M. Parniak, and E. S. Polzik, Phonon counting thermometry of an ultracoherent membrane resonator near its motional ground state, Optica **7**, 718 (2020).

[72] Z. Shen, Y.-L. Zhang, Y. Chen, C.-L. Zou, Y.-F. Xiao, X.-B. Zou, F.-W. Sun, G.-C. Guo, and C.-H. Dong, Experimental realization of optomechanically induced nonreciprocity, Nat. Photon. **10**, 657 (2016).

[73] C. Liu, Y. Sun, L. Zhao, S. Zhang, M. M. T. Loy, and S. Du, Efficiently loading a single photon into a single-sided Fabry-Perot cavity, Phys. Rev. Lett. **113**, 133601 (2014).

[74] S. Clark, A. Peng, M. Gu, and S. Parkins, Unconditional preparation of entanglement between atoms in cascaded optical cavities, Phys. Rev. Lett. **91**, 177901 (2003).

[75] G.-X. Li, H.-T. Tan, S.-P. Wu, and Y.-P. Yang, Entanglement for excitons in two quantum dots placed in two separate single-mode cavities, Phys. Rev. A **70**, 034307 (2004).

[76] Z. Li, S.-L. Ma, and F.-L. Li, Generation of broadband two-mode squeezed light in cascaded double-cavity optomechanical systems, Phys. Rev. A **92**, 023856 (2015).

[77] Q. Bin, X.-Y. Lü, S.-W. Bin, and Y. Wu, Two-photon blockade in a cascaded cavity-quantum-electrodynamics system, Phys. Rev. A **98**, 043858 (2018).

[78] C. W. Gardiner and P. Zoller, *Quantum Noise* (Springer, Berlin, 2000).

[79] Y.-F. Xiao, M. Li, Y.-C. Liu, Y. Li, X. Sun, and Q. Gong, Asymmetric Fano resonance analysis in indirectly coupled microresonators, Phys. Rev. A **82**, 065804 (2010).

[80] T. Li, T.-Y. Bao, Y.-L. Zhang, C.-L. Zou, X.-B. Zou, and G.-C. Guo, Long-distance synchronization of unidirectionally cascaded optomechanical systems, Opt. Express **24**, 12336 (2016).

[81] M. Zhang, S. Shah, J. Cardenas, and M. Lipson, Synchronization and phase noise reduction in micromechanical oscillator arrays coupled through light, Phys. Rev. Lett. **115**, 163902 (2015).

[82] J. Li, Z.-H. Zhou, S. Wan, Y.-L. Zhang, Z. Shen, M. Li, C.-L. Zou, G.-C. Guo, and C.-H. Dong, All-optical synchronization of remote optomechanical systems, Phys. Rev. Lett. **129**, 063605 (2022).

[83] E. Gil-Santos, M. Labousse, C. Baker, A. Goetschy, W. Hease, C. Gomez, A. Lemaître, G. Leo, C. Ciuti, and I. Favero, Light-mediated cascaded locking of multiple nano-optomechanical oscillators, Phys. Rev. Lett. **118**, 063605 (2017).

[84] A. Luis and J. Peřina, Contradirectional propagation and canonical transformations, Quantum Semiclass. Opt. **8**, 39 (1996).

[85] E. X. DeJesus and C. Kaufman, Routh-Hurwitz criterion in the examination of eigenvalues of a system of nonlinear ordinary differential equations, Phys. Rev. A **35**, 5288 (1987).

[86] G. Adesso, A. Serafini, and F. Illuminati, Extremal entanglement and mixedness in continuous variable systems, Phys. Rev. A **70**, 022318 (2004).

[87] R. Simon, Peres-Horodecki separability criterion for continuous variable systems, Phys. Rev. Lett. **84**, 2726 (2000).

[88] L. Gyongyosi and S. Imre, A survey on quantum computing technology, Comput. Sci. Rev. **31**, 51 (2019).

[89] E. Knill, Quantum computing with realistically noisy devices, Nature (London) **434**, 39 (2005).

[90] J. L. O'Brien, Optical quantum computing, Science **318**, 1567 (2007).

[91] C. L. Degen, F. Reinhard, and P. Cappellaro, Quantum sensing, Rev. Mod. Phys. **89**, 035002 (2017).

[92] K. A. Gilmore, M. Affolter, R. J. Lewis-Swan, D. Barberena, E. Jordan, A. M. Rey, and J. J. Bollinger, Quantum-enhanced sensing of displacements and electric fields with two-dimensional trapped-ion crystals, Science **373**, 673 (2021).

[93] S. Barzanjeh, S. Pirandola, D. Vitali, and J. M. Fink, Microwave quantum illumination using a digital receiver, Sci. Adv. **6**, eabb0451 (2020).

[94] W. Chen, Ş. K. Özdemir, G. Zhao, J. Wiersig, and L. Yang, Exceptional points enhance sensing in an optical microcavity, Nature (London) **548**, 192 (2017).

[95] S. L. N. Hermans, M. Pompili, H. K. C. Beukers, S. Baier, J. Borregaard, and R. Hanson, Qubit teleportation between non-neighbouring nodes in a quantum network, Nature (London) **605**, 663 (2022).

[96] C. Simon, Towards a global quantum network, Nat. Photon. **11**, 678 (2017).

[97] P. Kómár, E. M. Kessler, M. Bishof, L. Jiang, A. S. Sørensen, J. Ye, and M. D. Lukin, A quantum network of clocks, Nat. Phys. **10**, 582 (2014).

[98] H. Shen, X. Su, X. Jia, and C. Xie, Quantum communication network utilizing quadripartite entangled states of optical field, Phys. Rev. A **80**, 042320 (2009).

[99] K. V. Kheruntsyan, G. Yu. Kryuchkyan, N. T. Mouradyan, and K. G. Petrosyan, Controlling instability and squeezing from a cascaded frequency doubler, Phys. Rev. A **57**, 535 (1998).

[100] D. Roberts and A. A. Clerk, Driven-dissipative quantum Kerr resonators: New exact solutions, photon blockade and quantum bistability, Phys. Rev. X **10**, 021022 (2020).

[101] Y. H. Zhou, F. Minganti, W. Qin, Q.-C. Wu, J.-L. Zhao, Y.-L. Fang, F. Nori, and C.-P. Yang, n-photon blockade with an n-photon parametric drive, Phys. Rev. A **104**, 053718 (2021).